Available online at www.sciencedirect.com

ScienceDirect

Physics Procedia 84 (2016) 157 – 164

Physics Procedia

International Conference "Synchrotron and Free electron laser Radiation: generation and application", SFR-2016, 4-8 July 2016, Novosibirsk, Russia

Wave-vector spectrum of monochromatic terahertz surface plasmon polaritons on real surfaces

V.V. Gerasimov[a,*], B.A. Knyazev[a,b], A.K. Nikitin[b,c]

[a] *Budker Institute of Nuclear Physics, SB RAS, 630090 Novosibirsk, Russia*
[b] *Novosibirsk State University, 630090 Novosibirsk, Russia*
[c] *Scientific and Technological Center for Unique Instrumentation of RAS, 117342 Moscow, Russia*

Abstract

Experiments at the Novosibirsk free electron laser demonstrating that monochromatic terahertz surface plasmon-polaritons (SPPs) on a real metal surface have a rather wide-band spectrum of their wave-vector are described. The fact was evidenced by detection of bulk waves radiated from the SPP track and by means of SPPs reflection from a mirror installed normally to the sample surface or tilted to it. The cause of the wave-vector splitting is supposed to be SPPs scattering on imperfections of the surface. This splitting leads to substantial radiative losses of the SPPs, which may be the cause of violation of the $1/\omega^2$ SPP propagation length dependence predicted by the Drude model.

Peer-review under responsibility of the organizing committee of SFR-2016.

Keywords: surface plasmon polaritons; terahertz radiation; real metal surfaces; wave-vector spectrum

1. Introduction

At first sight the paper's title seems to be strange as namely monochromatic (not broad-band) surface plasmon polaritons (SPPs), a kind of surface electromagnetic waves, are considered. This puzzlement is justified in case of an ideal homogenous "metal-dielectric" interface when the SPP wave-vector spectrum represents itself just a line which location on the wave-vector axis is defined by the bordering media dielectric constants (ε_1 and ε_2) and the radiation frequency ω (Raether, 1988):

* Corresponding author. Tel.: +7-383-339-48-39; fax: +7-383-330-32-35.
E-mail address: einy@ngs.ru

Peer-review under responsibility of the organizing committee of SFR-2016.
doi:10.1016/j.phpro.2016.11.028

$$k_{SPP} = \frac{\omega}{c} \cdot \sqrt{\frac{\varepsilon_1 \cdot \varepsilon_2}{\varepsilon_1 + \varepsilon_2}}\,, \tag{1}$$

here c is the speed of light in the dielectric.

It is a different matter in case SPPs propagate along a real "metal-dielectric" interface containing both roughness and material imperfections (intrusions and/or grains of the metal). On running these imperfections SPPs gain a wide spectrum of an additional momentum characteristic to the metal surface inhomogeneities that leads to a rather wide wave-vector spectrum of the SPPs in spite of their monochromatic character. Some of the harmonic components of the spectrum are greater than k_{SPP}, others are less. It may occur that some of the latter ones are less than the plane wave vector $k_o = \omega/c$ in air, which makes the SPPs to be radiative. This is the origin of SPP radiative losses increasing attenuation of the SPPs by complimenting the Joule losses (Raether, 1988).

Results on investigations of the wave-vector composition of monochromatic (wavelength λ=130 μm) THz SPPs on evaporated gold samples are presented in the paper. Existence of a SPP wave-vector broad-band spectrum was evidenced in the two ways: 1) by detecting bulk radiation emitted from the SPP track; 2) by measuring the dependence of SPPs reflection from a plane mirror installed on the sample surface versus the angle of the mirror deflection from the normal to the surface.

2. Brief theory

2.1. On the possible role of the SPP radiative losses at terahertz frequencies

SPPs are inherently nonradiative surface waves as the real part k'_{SPP} of their wave vector $k_{SPP} = k'_{SPP} + i \cdot k''_{SPP}$ (where i is the imaginary unit) exceeds the wave vector k_o of a plane wave in free space (air). However, when the guiding interface has roughness or intrinsic impurities, SPPs lose their nonradiative nature and acquire additional losses, referred to as "radiative" due to their origin (Raether, 1988). Imperfections of the surface add an increment $\Delta k = \Delta k' + i \cdot \Delta k''$ to the wave vector k_{SPP}. Note that the value of Δk is not strictly defined; it is distributed over a relatively large span, reaching maximum at its centre. If $\Delta k'$ is negative (in case the SPP wave vector k_{SPP} and the imperfection impact Δk are oppositely directed), it may result in the inequality

$$k'_{SPP} - |\Delta k'| \le k_0\,, \tag{2}$$

thus making the SPPs to be radiative and running a shorter distance as compared with the case of an ideal plane interface.

In the visible range, the dispersion curve $k_{SPP}(\omega)$ is spaced from the light line $k_o(\omega)$ by a rather large distance (along the k-axis) mainly exceeding the most probable value of $\Delta k'$, which results in relatively small radiative losses of the SPPs. However, with an increase in λ, the dispersion curve comes closer and closer to the light line, making the transformation of SPPs into bulk waves on surface imperfections more and more probable. It means that at low frequencies, particularly in the THz range, the role of radiative losses in total SPP attenuation on a real interface is expected to increase. That may be the reason, why the SPP propagation length does not obey the $1/\omega^2$ dependence as the Drude model for the metal dielectric permittivity predicts.

2.2. On reflection of monochromatic terahertz SPPs by a plane mirror

Suppose a plane mirror is installed on a sample surface guiding SPPs. Such an "obstacle" may be considered as an imperfection of the surface. Due to the SPP-mirror interaction the wave vector k_{SPP} gains a negative increment Δk. If the mirror is oriented normally to the surface than, in accordance with the momentum conservation law, $\Delta k' = -2k'_{SPP}$ and the SPPs are simply reflected backwards like a plane wave, provided the penetration depth of their

field into air exceeds 3λ (Bell et al., 1975). But what will happen in case the mirror is deflected to an angle α from the normal? Will the SPPs obey the law of reflection or transform into a plane wave radiated into the adjacent medium? And what role the wave-vector ambiguity plays in the process of SPPs reflection from a mirror? All these problems remain still unresolved.

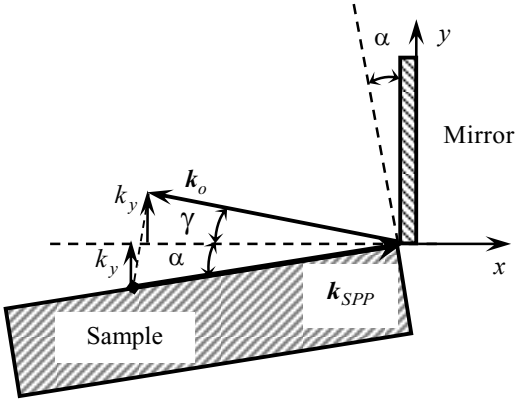

Fig. 1. Transformation of SPPs into a plane wave on its reflection from a plane mirror deflected to the angle α from the normal to the sample surface.

So, let us first consider the problem of SPP reflection from a mirror deflected to an angle α from the normal to the sample surface analytically. To facilitate understanding of the situation, suppose that the sample is turned anticlockwise to an angle α from the horizontal line, while the mirror remains its vertical position (Fig.1). Under these conditions the SPP wave vector has two rectangular components relative to the mirror: $k_x = k'_{SPP} \cdot \cos(\alpha)$ and $k_y = k'_{SPP} \cdot \sin(\alpha)$. There are two possible outcomes of the SPP-mirror interaction depending on the k_x value: in case $k_x > k_o$ the reflected radiation preserves the nature of SPPs; in case $k_x < k_o$ the SPPs convert into a plane wave, radiated into air at an angle $\gamma > \alpha$ relative the *x*-axis. The angles are different as *y*-components of the vectors $\boldsymbol{k}_{SPP}$ and $\boldsymbol{k}_o$ are equal due to the momentum conservation law, but their modules are not equal ($|\boldsymbol{k}_{SPP}| > |\boldsymbol{k}_o|$). Therefore, as the mirror deflection angle α is being increased the transformation of the SPPs into a plane wave takes place not under the condition $k_x = k_o$, but when the equality $k_x = k_o \cdot \cos(\gamma)$ is achieved.

Let us express k'_{SPP} via the angles α and γ. To do this we shall take advantage of vectors $\boldsymbol{k}_{SPP}$ and $\boldsymbol{k}_o$ *y*-components equality: $k_y = k'_{SPP} \cdot \sin(\alpha) = k_o \cdot \sin(\gamma)$. Whence it follows that:

$$k'_{SPP} = k_o \cdot \sin(\gamma) / \sin(\alpha). \tag{3}$$

In view of the fact that measurement of the both angles is a rather laborious process, let us try to obtain an approximate formula for k'_{SPP} estimation from the value of angle α_{max} corresponding to transformation of the SPPs into a plane wave. To do this one has to take into account the following facts: first, according to (3) the SPP refractive index $\kappa' \equiv k'_{SPP}/k_o = \sin(\gamma)/\sin(\alpha)$; second, the angles α and γ are small; third, value of κ' for a "metal-air" interface at THz frequencies does not exceed 1.001, this enables us to consider that the difference (γ-α)≤10″ and therefore angles α and γ are approximately equal. Under these conditions one may state that projection of vector $\boldsymbol{k}_{SPP}$ on the direction of propagation of the plane wave produced by the SPPs due to their interaction with the mirror should equal k_o. Then, as it follows from Fig. 1, $k_o/k'_{SPP} \approx \cos(2\alpha_{max})$, wherefrom:

$$k'_{SPP} \approx k_o / \cos(2\alpha_{max}). \tag{4}$$

3. Experimental setups

To obtain the both experimental evidences that monochromatic SPPs have a rather broad-band spectrum of the wave vector we assembled two relevant setups.

The schematic of the first one aimed at detection of bulk waves (BWs) emitted from the SPP track is shown in Fig. 2. A *p*-polarized Gaussian beam of the Novosibirsk free-electron laser, FEL, (Kulipanov et al., 2015) with λ=130 μm entered the setup as a stream of 100-ps pulses with a 5.6 MHz repetition rate and an average power of about 10 W. Polarizers Pol 1 and Pol 2 were applied for beam attenuation and polarization control, accordingly. The input beam intensity was monitored using a beam splitter BS with a pyroelectric sensor. To transform the radiation into SPPs we employed the end-fire coupling technique (Stegeman et al., 1983). But in contrast to the classical implementation of the method with a sample rectangular edge, we used a one-eighth part of a glass cylinder, its optical-quality polished curved surface covered with a 1-μm thick gold film, as a coupling element (Nikitin et al., 2012). The cylindrical form of the element made it an effective screen, shielding the photo detector from diffracted BWs. The radius of the cylinder, R=60 mm, exceeded λ manifold, which made the curvature contribution to the radiative losses negligible. To increase the coupling efficiency, we covered the gold film with a 2 μm thick *ZnS* layer. The generated SPPs proceeded from the cylindrical surface of the element to the sample plane surface adjoining it.

BWs emitted from the track due to the interaction of the SPPs with surface imperfections were reflected by a 45° inclined plane mirror and detected with a TPX lens and an optoacoustic detector (a GC-1D Golay cell). The cell was coupled to a lock-in amplifier SR-830 tuned at a 15 Hz chopping frequency. The mirror, the detector and the lens were placed on an optical rail in *f-f* arrangement, where f=100 mm is the focal length. The detector was equipped with a 0.2 mm diaphragm (oriented normally to the plane of incidence), cutting off parasitic BWs. In addition, the detector was shielded with an accessory metal screen from BWs generated by the SPPs due to their diffraction on the junction between the coupling element and the sample. The screen was fixed over the SPP track, its edge in 15 mm from the junction and 10 mm from the sample surface. The detector was scanned in the focal plane along the *y*-axis, and the patterns of bulk radiation emitted by the SPPs due their interaction with the surface imperfections were recorded (see Sec. 4.1).

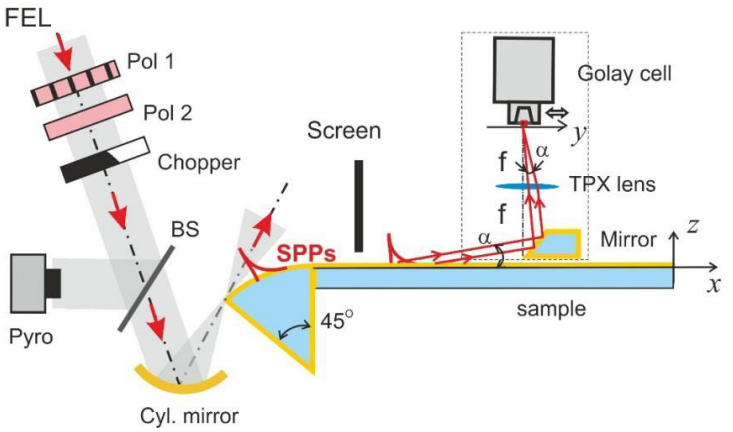

Fig. 2. Experimental setup with the end-fire coupling technique to excite SPPs on the edge of a cylindrical coupling element attached to a plane-surface sample for sensing bulk waves emitted from the SPP track.

The schematic of the second setup used for measuring the dependence of SPPs reflection from a plane mirror, is displayed in Fig. 3. Now we employed two cylindrical coupling elements (to couple and decouple the SPPs) and a plane mirror (40×40 mm^2) installed on the sample surface and crossing the SPP track at an angle β=45°. The mirror was provided with two axes: one – to control the angle β, the other – to change the angle α of the mirror deflection

from the normal $\boldsymbol{n}$.

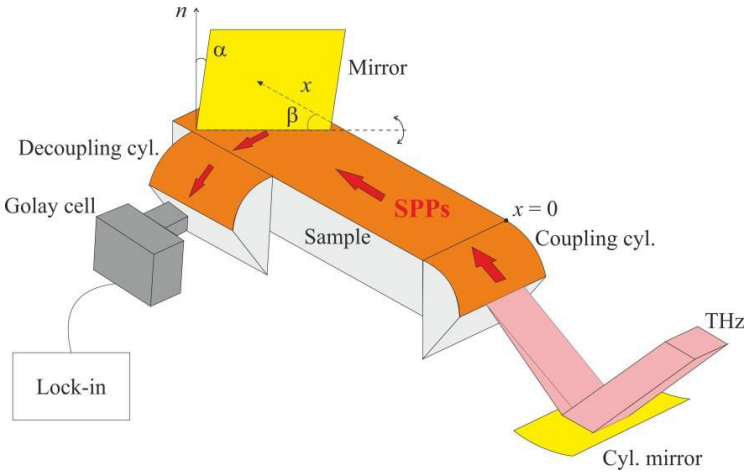

Fig. 3. Schematic of the setup used for study of reflection of SPPs from a plane mirror.

The samples were 15.0×3.5×1.0 cm^3 glass substrates with their top faces 15.0×3.5 cm^2 being optically polished and covered with an opaque 0.3 μm thick film of gold. Zink sulfate (*ZnS*) layer of optional thickness varying from zero to 0.7 μm was deposited on the gold film.

4. Experimental evidences of SPPs wave vector broad-band spectrum existence

4.1. Detection of wide-spread bulk radiation from the SPP track

Detection of bulk waves (BWs) emitted from the track in various directions due to conversion of the SPPs on imperfections of the surface is a substantial argument in favor of SPPs wave vector broad-band spectrum existence. On assuming that these BWs are emitted at rather small angles to the SPP track, we put a 45° inclined plane mirror right on the sample surface at the distance $x \approx 150$ mm from the "coupling element – sample" junction. Scanning the detector along the *y*-axis in the focal plane of the lens, we measured the angular spectrum of the radiation coming from the reflecting facet of the mirror. The angular distributions of the incoming radiation recorded for the samples with *ZnS* layers of thickness d=0.0, 0.4 and 0.7 μm are shown in Fig. 4. Each individual diagram recorded for a given sample had two main maxima (a subsidiary maximum was observed only for the sample with d=0.70 μm).

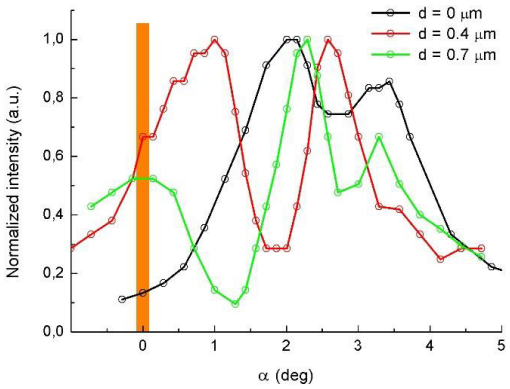

Fig. 4. Radiation patterns recorded from the SPP track on gold samples with *ZnS* layer of various thicknesses *d*.

The first maximum (observed in the angular span $\alpha=(0\div2)°$, where α is the angle counted from the sample surface to the BW wave vector, as well as the third one for the sample with d=0.70 μm at $\alpha\approx3.5°$, corresponded to BWs produced by the SPPs due to their diffraction on the front edge of the mirror. Similar radiation patterns were observed for SPPs diffracting on a sample rectangular edge (Gerasimov et al., 2013), which is an evidence of the diffractional nature of the SPP transformation on the mirror edge.

The second maximum (at greater α) was formed by BWs produced by the SPPs on their track due to interaction with surface imperfections. To make sure that it was really produced by BWs incident on the 15-mm long reflecting facet of the mirror and that it had a "radiative" nature, we put a paper strip 2.5 mm wide horizontally on the facet and moved it gradually downwards to the sample surface (see Fig. 5). Further we describe the observed changes in the maxima when the strip was being moved downwards to the sample with *ZnS* layer 0.40 μm thick. As soon as the strip was put on the upper edge of the facet of the mirror, the second maximum started decreasing, and when the strip passed one third of the facet length (position A in Fig. 5), its intensity was four times as small as the initial value. Up to this position, the first SPP maximum remained unchanged. Further shifting of the strip towards the lower edge of the mirror led to a gradual increase in the second maximum and a decrease in the first one. At the terminal point of the strip motion, when it touched the sample surface (position B in Fig. 5), the second maximum was half of its initial value, while the first maximum reached its minimum, about a one third of its initial value. Such behavior of the maxima evidences the existence of BWs emitted from the SPP track and propagating at an angle α with the sample surface. It is worth noting that with the *ZnS* layer thickness growing the second maximum shifts to the normal ($\alpha=0°$) like the first one, which indicates an increase in the SPP wave vector with thicker coatings.

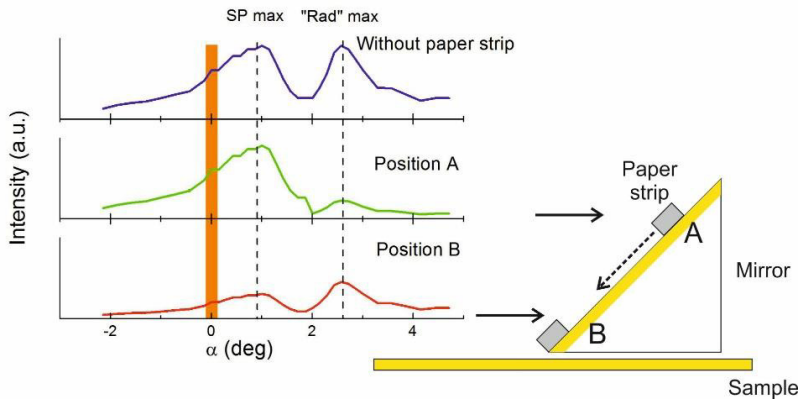

Fig. 5. Testing "radiative" nature of the second maximum: experimental scheme and results for the sample with *ZnS* layer 0.4 μm thick. The traces were recorded with a Golay cell placed at a motorized translation stage.

4.2. SPP wave-vector spectrum manifestation in reflection of SPPs from a plane mirror

Results of the experiments on reflection of THz SPPs by a plane mirror, disposed at distance $x\approx50$ mm from the junction "coupling element – plane sample", are presented in Fig.6. Coefficient of reflection $R = I/I_o$ (I_o is output signal from the detector in case the mirror reflecting facet contains the normal to the sample surface, i.e. $\alpha=0$) is plotted on the ordinate axis. The reflection coefficient estimation error ΔR was supposed to equal 10% and was mainly caused by the FEL radiation instability.

Analysis of the obtained dependencies $R(\alpha)$ enabled us to make the following conclusions: 1) the SPP reflection coefficient drops to zero not at a definite angle $\alpha=\alpha_{max}$ as it follows from formula (4), but it vanishes gradually, that indirectly evidences a multivaluedness of the SPP wave vector (angle α_{max} ambiguity, caused by the 1% radiation line width of the FEL, did not exceed 1′); 2) the SPP reflection coefficient starts to decrease in reality at an angle $\alpha^*<\alpha_{max}$, which again evidences in favour of multivaluedness of the SPP wave vector; 3) value of angle α^* is proportional to the *ZnS* layer thickness making plots of $R(\alpha)$ broader, which may be interpreted as widening of the SPP wave vector spectrum.

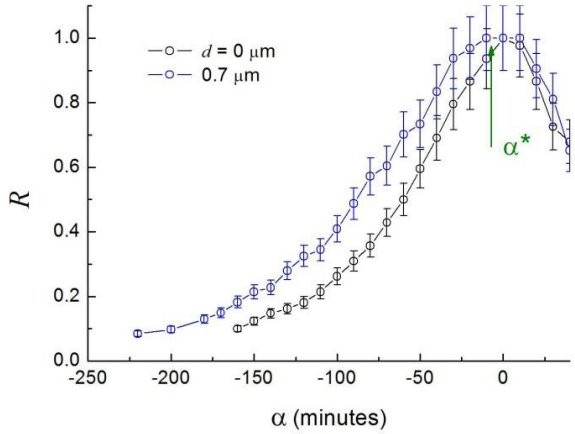

Fig. 6. Experimental dependencies of the SPP reflectance *R* by a plane mirror on its angle of deflection α from the normal to the sample surface measured for bare (circles) and covered with 0.7 μm thick *ZnS* layer (triangles) gold specimens.

The wave-vector spectrum of SPPs on a real interface may be estimated from the experimental data employing the following approximate formula:

$$k' \approx k_o / \cos(2\alpha) = k_o / \{\cos[2 \cdot (\alpha^* + \Delta\alpha)]\}, \quad (5)$$

where α* is the measured maximal angle of the mirror deflection at which intensity of the reflected SPPs equals their intensity for a normally installed mirror, i.e. at α=0°; Δα is an additive to α* originating from scattering of the SPPs on roughness and impurities of the metal surface.

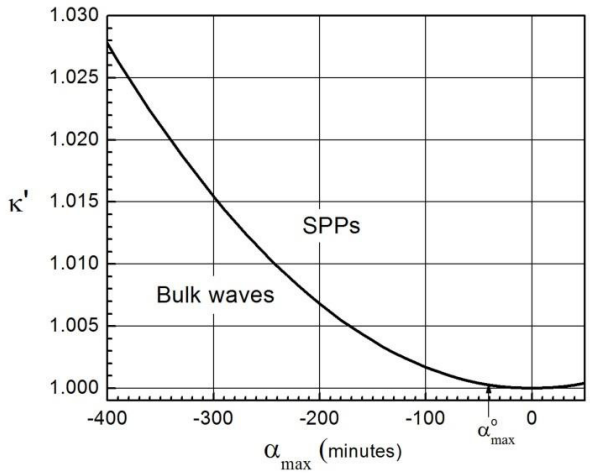

Fig. 7. Calculated dependence of the SPP refractive index κ' on the angle α_{max} of deflection of a plane mirror reflecting the SPPs from the normal to the sample surface, corresponding to transformation of the SPPs into a plane wave.

To estimate the wave-vector spectrum of SPPs on a real interface one has to compare the dependence $\kappa'(\alpha_{max})$, calculated with formula (4) and having nothing in common with any waveguiding structure, and the dependence $R(\alpha)$, measured for the interface concerned. The plot of the $\kappa'(\alpha_{max})$ is presented in Fig.7. Area above the curve $\kappa'(\alpha_{max})$ corresponds to preservation of the mirror-reflected SPPs of their nature; area below the curve corresponds to transformation of the mirror-reflected SPPs into a plane wave radiated into air at an angle $\alpha \leq 2\alpha_{max}$.

Matching each value of angle α on a graph like that presented in Fig.6 to a certain value of κ' in Fig.7, it is easy to determine the whole spectrum of κ' values. For example, as maximum values of angle α at which the reflected SPPs were still detected (R>0) for the samples with d=0 and d=0.7 μm were 160′ and 225′, one may state that maximum values of κ' for SPPs on these samples were 1.004 and 1.008, accordingly.

We have every reason to assume that namely this ambiguity of the SPP wave vector, originating from scattering of the SPPs on imperfections of a real metal surface, is the cause of unexpectedly large radiative losses not only in the middle IR, but in the THz range as well.

5. Conclusion

The investigations described in the paper obviously confirm that the wave vector of monochromatic surface plasmon-polaritons (SPPs) on a real metal surface have a rather wide-band spectrum of their wave-vector. This fact was evidenced by two kinds of experiments performed with terahertz SPPs excited by free-electron laser radiation on gold samples: 1) direct detection of bulk waves (BWs) emitted by the SPPs from their track; 2) reflection of SPPs by a mirror installed across the SPP track and capable to change its deflection from the normal to the sample surface. Both, the emitted BWs radiation pattern and the mirror tilt angle insuring reflection of the SPPs, had a similar angular span, validating that the SPPs had a wide spectrum of their wave vector. We consider that this widening of the spectrum occurs due to scattering of SPPs on imperfections of various kinds embedded by the metal surface. As some of the spectrum components may be less than the plane wave vector in air, the SPPs lose their nonradiative nature and gain radiative energy losses complimenting the Joule ones. That may be the cause of the phenomenon that SPP propagation length does not obey the $1/\omega^2$ dependency predicted by the Drude model.

Acknowledgments

The equipment belonging to the Siberian Synchrotron and Terahertz Radiation Center was used in the experiments. The development and assembly of dedicated terahertz focusing system (beamline) was supported by Russian Science Foundation (grant 14-50-00080). The work was supported in parts by the Russian Foundation for Basic Research grant No.16-32-00678 and by the Fundamental Scientific Research project No. 0069-2014-0014 (RAS).

References

Bell, R. J., Goben, C. A., Davarpanah, M., Bhasin, K., Begley, D. L., Bauer, A. C., 1975. Two-dimensional optics with surface electromagnetic waves. Appl. Optics, 14 (6), 1322-1325.

Gerasimov, V. V., Knyazev, B. A., Kotelnikov, I. A., Nikitin, A. K., Cherkassky, V. S., Kulipanov, G. N., Zhizhin, G. N., 2013. Surface plasmon polaritons launched using a terahertz free electron laser: propagating along a gold-*ZnS*-air interface and decoupling to free waves at the surface tail end. J. Opt. Soc. Am. (B) 30, 2182-2190.

Kulipanov, G.N., Bagryanskaya, E.G., Chesnokov, E.N., Choporova, Y.Yu, Gerasimov, V.V., Getmanov, Ya.V., Kiselev, S.L., Knyazev, B.A., Kubarev, V.V., Peltek, S.E., Popik, V.M., Salikova, T.V., Scheglov, M.A., Seredniakov, S.S., Shevchenko, O.A., Skrinsky, A.N., Veber, S.L., Vinokurov, N.A. 2015. Novosibirsk free electron laser—facility description and recent experiments. IEEE Transactions on Terahertz Science and Technology 5, 798-809.

Nikitin, A. K., Zhizhin, G. N., Knyazev, B. A., 2012. A device to measure the propagation length of monochromatic surface electromagnetic waves of the infrared spectral range. Patent of Russia on invention No.2470269, Bull. 35.

Raether, H., 1988. Surface plasmons on smooth and rough surfaces and on gratings. *Springer Tracts in Modern Physics* 111 (Springer-Verlag).

Stegeman, G. I., Wallis, R. F., Maradudin, A. A., 1983. Excitation of surface polaritons by end-fire coupling. Optics Lett. 8 (7), 386-388.